Results and Discussion

AhR ligand activity was examined with both a mouse hepatoma (H1L1) cell system and a yeast system for fractions separated from DMSO solution of extracts of road dust and DEPs, using reversed-phase (ODS) HPLC (Fig. 1). In the road dust extract (equivalent to ~1 mg), the polar region (fractions ≤ 30) as well as the hydrophobic region (approximately fractions 31–45) contributed to total AhR ligand activity in the H1L1 cell system. Significant activities were observed in several much later fractions (fractions > 45). Several AhR ligand active compounds including high-ring PAHs or natural compounds, with later retention times and derived from tires or asphalt, also may contribute to the AhR ligand activity of road dust (Rogge et al. 1993b). The contribution of the region including

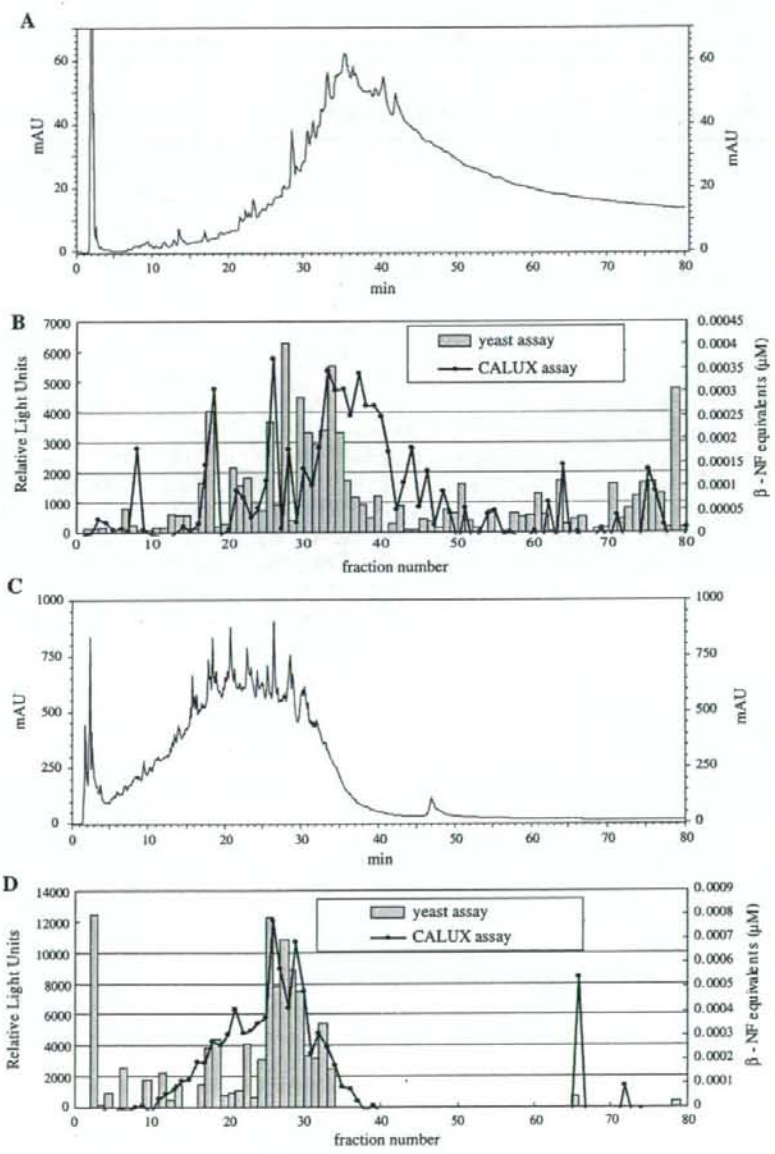

Fig. 1 AhR activities in yeast assay and CALUX assay for exposure to each fraction separated on an ODS column from extracts of road dust and diesel exhaust particulates (β-NF equivalents for yeast assay and relative light units for CALUX assay). A UV absorption for road dust. B AhR ligand activity for road dust. C UV absorption for diesel exhaust particulates. D AhR ligand activity for diesel exhaust particulates

PAHs to the total AhR ligand activity was higher in the H1L1 system than in the yeast system. This is probably because the speed of uptake and metabolism of hydrophobic contents (such as PAHs) are slower for yeast than for mouse hepatoma cells (Miller et al. 1999; Misaki et al. 2007b). However, in DEP extract (equivalent to ~100 μg), fractions with later retention times (fractions ≥ 40) did not show significant AhR ligand activity except for fractions 66 and 72. It was observed that polar compounds were included relatively more in DEP extract than in road dust extract, by the strength of UV absorption in each fraction. This may be because oxy-PAHs generated from automobiles are decomposed on the road more easily than PAHs, while DEPs include various oxy-PAHs (Rogge et al. 1993a).

Moreover, minute separation of the constituents of the dichloromethane extract of road dust was carried out using Sephadex (LH20), normal-phase (silica gel), and reversed-phase (ODS) column HPLC, in that order (Fig. 2). AhR ligand activity in yeast assay and ER ligand activity in Chinese hamster ovary (CHO-1) cell assay were examined for the fractions in the separation. In the first separation for the extract of road dust, 20 mg with Sephadex HPLC, neither AhR nor ER ligand activity was found, but significant UV absorption was detected in fractions with early retention times (fractions 1–4), while both activities were observed in later fractions (Fig. 3). Nonactive aliphatic hydrocarbons, aliphatic acids, low-ring-number PACs, and so on are probably removed as early-eluted components by this method (Casellas et al. 1995). In addition, for the residue in evaporation of active fractions (fractions 5–20; 12 mg), separation with normal-phase HPLC and AhR and ER assay of these fractions were performed (Fig. 4). Retention times of representative PACs in this normal-phase HPLC were also examined (Table 1), although the concentration of each PAC was not examined in this study. The existence of these PACs in road dust is fully expected from analytical data previously reported for atmospheric environments (Rogge et al. 1993a; Alsberg et al. 1985; Casellas et al. 1995; Hannigan et al. 1998; Pedersen et al. 2005; Fernandez et al. 1992). In the second separation of road dust extract using normal-phase HPLC, the AhR ligand active peak was observed in fraction 8–11, where many PAH standards are included in the same fractions. Weak ER ligand activity was shown in fraction 8–11, and this is thought to be generated from PAHs such as B[a]P, benz[*a*]anthracene, and chrysene, showing weak ER ligand activity (Machala et al. 2001b; Clemons et al. 1998). AhR ligand activity observed in fractions 12–19 was probably derived from PAKs and PAQs (they were thought to be contained in these fractions; Table 1). AhR ligand activity was also observed in fractions 20–50, and remarkable ER ligand activity was observed in the region of fractions 37–43 and 48–54. It has not been determined what compounds contribute to the AhR and ER ligand activity in fractions 37–43. Hydroxy-PAHs are candidates contributing to these activities in these fractions because several hydroxy-PAHs have both AhR and ER ligand activity (Kamiya et al. 2005; Hirose et al. 2001; van Lipzig et al. 2007; Burczynski et al. 2000). It has not been elucidated what compounds contribute to the ER ligand activity of fraction 48–54. Polycyclic aromatic carboxylic acids, estradiol derived from natural compounds, and possibly hydroxylated cyclic aliphatic hydrocarbons like estradiol are candidates for ER ligand activity in these fractions (Hannigan et al. 1998; Casellas et al. 1995; Fernandez et al. 1992; Kamiya et al.

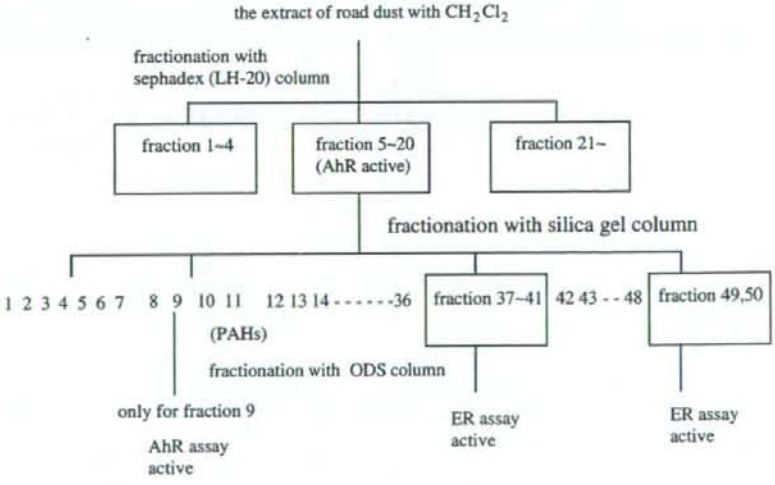

Fig. 2 Flow of the separation of extracts of road dust and AhR and ER assays for fractions

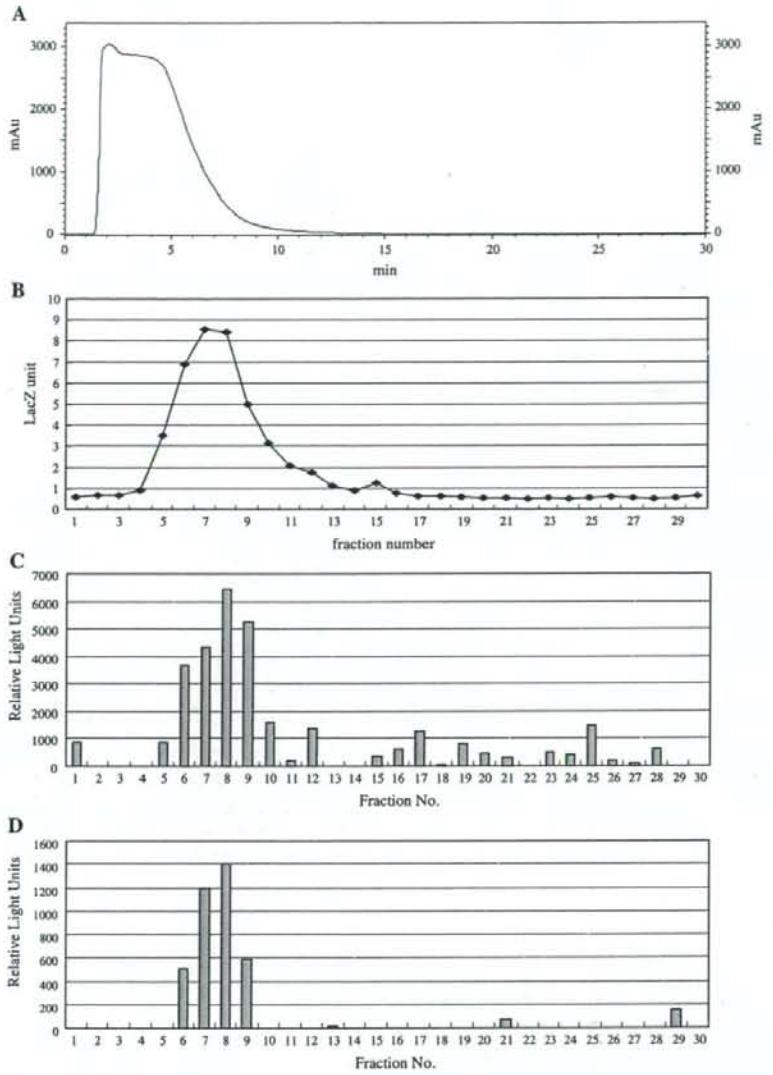

Fig. 3 First separation of extracts of road dust with a Sephadex column and bioassay of fractions. A UV absorption at 254 nm. B AhR assay. C ER α assay. D ER β assay

2005; van Lipzig et al. 2005). Further separation of fraction 9 with reversed-phase HPLC was performed and a clear UV chromatogram was observed at the retention times including PAHs (Fig. 5).

It was reported that the formation of many kinds of oxy-PAHs were observed in the oxidation process of PAHs (Nikolaou et al. 1984; Letzel et al. 2001; Choi et al. 2003), and the toxicological significance of polar compounds in environments is predicted (Matsumoto et al. 1986; Kannan et al. 2000; Clemons et al. 1998; Choi et al. 2003). In our previous study AhR ligand activities of oxy-PAHs such as PAKs and PAQs are lower than representative AhR ligand active PAHs (benzo[*k*]fluoranthene, dibenz[*a*,*h*]anthracene, B[a]P etc.), and the calculated contribution of representative PAKs and PAQs to AhR ligand activity in atmospheric samples was estimated to be significant but not very much (Misaki et al. 2007b). However, considering the contribution of polar fractions to the total AhR ligand activity of road dust and DEPs in the present study, it is probable that several polar compounds such as aliphatic acids, hydroxy-

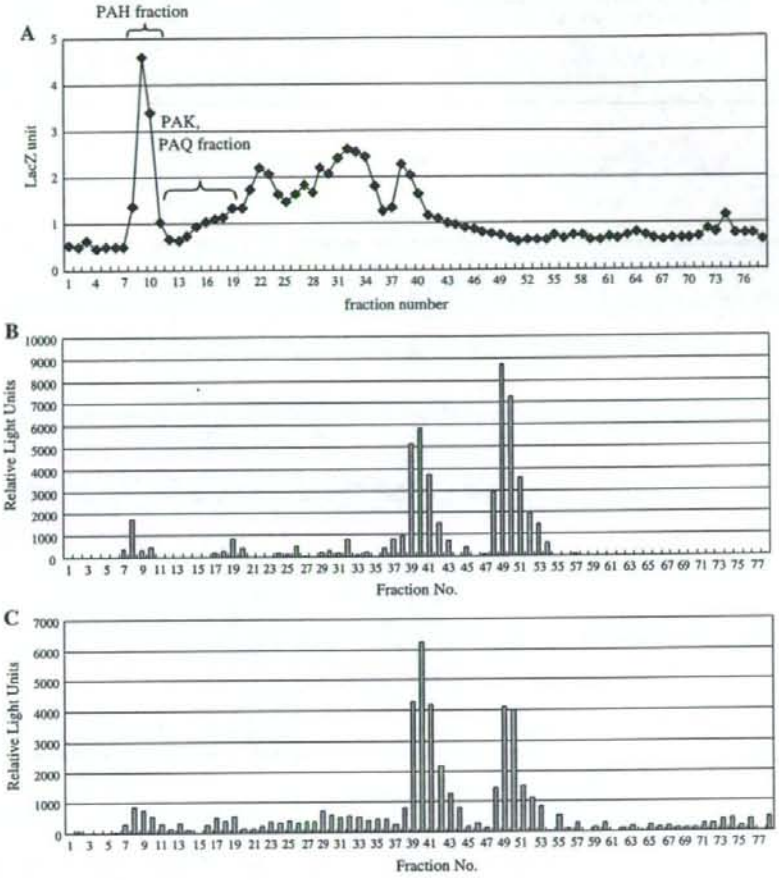

Fig. 4 Second separation of extracts of road dust with a silica gel column and bioassay of fractions. A AhR assay. B ER α assay. C ER β assay

PAHs, polycyclic aromatic carboxaldehydes, polycyclic aromatic carboxylic acids, and polycyclic aromatic anhydrides have significantly potent AhR ligand activity and contribute to the AhR ligand activity of road dust and DEPs (Binková et al. 1998; Casellas et al. 1995; Rogge et al. 1993a, b).

Consequently, AhR ligand activity was confirmed in the extracts of both road dust and DEPS. In the separation of the extracts of both road dust and DEPs with reversed-phase HPLC, it was found that polar fractions contributed to significant AhR ligand activity both in the mouse hepatoma (H1L1) cell system and in the system. Furthermore, the contribution of these polar fractions was higher in DEPs than in road dust. The contribution of the polar region to AhR ligand activity was also observed with the separation of road dust extract by normal-phase HPLC. Additionally, remarkable ER ligand activity was confirmed in the highly polar region separated by normal-phase HPLC. The identification of unknown AhR or ER ligand active compounds and their detailed analysis in the polar region are problems for future study.

Acknowledgments We thank Dr. Charles A. Miller III of the Department of Environmental Health Sciences and the Tulane-Xavier Center for Bioenvironmental Research, Tulane University School of Public Health and Tropical Medicine, New Orleans, Louisiana, for kindly supplying us with the YCM3 strain. We acknowledge the Shiga National Highway Construction Work Office, Kinki Regional Construction Agency, Ministry of Construction, and Ritto Management Office, Nagoya Management Agency, Japan Highway Public Corp., for their cooperation in collection of road dust; Dr. Yoshihisa Shimizu, Research Center for Environmental Quality Management, Kyoto University, for kindly allowing us to use the ASE instrument; and Dr. Ryoichi Kizu, Faculty of Pharmaceutical Sciences, Doshisha Woman's College of Liberal Arts, Kyoto, for kindly providing us with diesel particulates. We also thank Hirofumi Kawami and Tota Tanaka, Research Center for Environmental Quality Management, Kyoto University, and Dr. Byung-Cheol Lee, Department of Environment Research, Korea Institute of Construction Technology, for

Table 1 Retention times of representative PACs in normal-phase HPLC

Retention time	Compound
6–8 min	Naphthalene
	Anthracene
8–11 min	Indeno[1,2,3-*c,d*]pyrene
	Pyrene
	Benzo[*a*]pyrene
	Benzo[*k*]fluoranthene
	Dibenz[*a,h*]anthracene
	Triphenylene
	Benz[*a*]anthracene
	Chrysene
11–19 min	7,12-Benz[*a*]anthracenequinone
	Benzo[*b*]fluoranthene
	1-Pyrenecarboxilic acid
	1-Pyrenecarboxaldehyde
	5,12-Naphthacenequinone
	Anthraquinone
	11*H*-Benzo[*a*]fluorene-11-one
	6*H*-Benzo[*cd*]pyrene-6-one
	11*H*-Benzo[*b*]fluorene-11-one
	Acridine
	Phenalenone
31 min	1-Hydroxypyrene

their assistance. This work was supported in part by Grants-in-Aid for Scientific Research (13027245, 16201012) from the Japanese Ministry of Education, Science, Sports and Culture.

References

Adachi J, Mori Y, Matsui S, Takigami H, Fujino J, Kitagawa H, Miller III CA, Kato T, Saeki K, Matsuda T (2001) Indirubin and indigo are potent aryl hydrocarbon receptor ligands present in human urine. J Biol Chem 276:31475–31478

Alsberg T, Strandell M, Westerholm R, Stenberg U (1985) Fractionation and chemical analysis of gasoline exhaust particulate extracts in connection with biological testing. Environ Int 11:249–257

Binková B, Lenícek J, Beneš I, Vindová P, Gajdoš O, Fried M, Šrám RJ (1998) Genotoxicity of coke-oven and urban air particulate matter in in vitro acellular assays coupled with ^{32}P-postlabeling and HPLC analysis of DNA adducts. Mutat Res 414:77–94

Bols NC, Schirmer K, Joyce EM, Dixon DG, Greenberg BM, Whyte JJ (1999) Ability of polycyclic hydrocarbons to induce 7-ethoxyresorfin-o-deethylase activity in a trout liver cell line. Ecotoxicol Environ Saf 44:118–128

Burczynski ME, Penning (2000) Genotoxic polycyclic aromatic hydrocarbon ortho-quinones generated by aldo-keto reductases induce CYP1A1 via nuclear translocation of the aryl hydrocarbon receptor. Cancer Res 60:908–915

Casellas M, Fernandez P, Bayona JM, Solanas AM (1995) Bioassay-directed chemical analysis of genotoxic components in urban airborne particulate matter from Barcelona (Spain). Chemosphere 30:725–740

Choi J, Oris JT (2003) Assessment of the toxicity of anthracene photo-modification products using the topminnow (Poeciliopsis lucida) hepatoma cell line (PLHC-1). Aquat Toxicol 65:243–251

Chou P-H, Matsui S, Matsuda T (2006) Detection and identification of dyes showing AhR-binding affinity in treated sewage effluents. Water Sci Technol 53(11):35–42

Chou P-H, Matsui S, Misaki K, Matsuda T (2007) Isolation and identification of xenobiotic aryl hydrocarbon receptor ligands in dyeing wastewater. Environ Sci Technol 41:652–657

Clemons JH, Allan IM, Marvin CH, Wu Z, McCarry BE, Bryant DW, Zacharewski TR (1998) Evidence of estrogen- and TCDD-like activities in crude and fractionated extracts of PM_{10} air

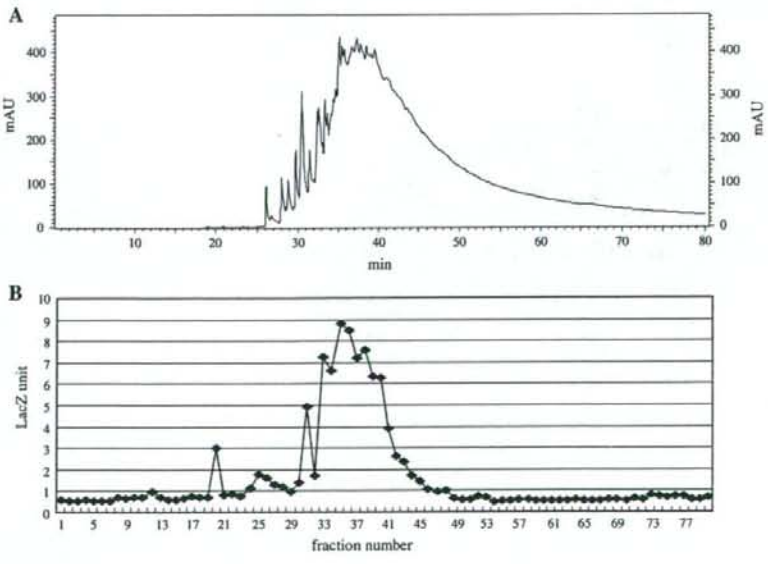

Fig. 5 Third separation with ODS column of fraction 9 in separation with silica gel column and AhR assay for fractions. A UV absorption with 254 nm. B AhR assay

particulate material using in vitro gene expression assays. Environ Sci Technol 32:1853–1860
Colborn T (2004) Endocrine disruption overview: Are males at risk? Adv Exp Med Biol 545:189–201
Crepineau C, Rychen G, Feidt C, Le Roux Y, Lichtfouse E, Laurent F (2003) Contamination of pastures by polycyclic aromatic hydrocarbons (PAHs) in the vicinity of a highway. J Agr Food Chem 51:4841–4845
Denison M, Brouwer A, Clark G (1998) U.S. patent 5,854,010
Denison MS, Pandini A, Nagy SR, Baldwin EP, Bonati L (2002) Ligand binding and activation of the Ah receptor. Chem-Biol Interact 141:3–24
Durant JL, Busby WF Jr, Lafleur AL, Penman BW, Crespi CL (1996) Human cell mutagenicity of oxygenated, nitrated and unsubstituted polycyclic aromatic hydrocarbons associated with urban aerosols. Mutat Res 371:123–157
Fernandez P, Bayona JM (1992) Use of off-line gel permeation chromatography-normal-phase liquid chromatography for the determination of polycyclic aromatic compounds in environmental samples and standard reference materials (air particulate matter and marine sediment). J Chromatogr 625:141–149
Giesy JP, Hilsherova K, Jones PD, Kannan K, Machala M (2002) Cell bioassays for detection of aryl hydrocarbon (AhR) and estrogen receptor (ER) mediated activity in environmental samples. Mar Poll Bull 45:3–16
Hannigan MP, Cass GR, Penman BW, Crespi CL, Lafleur AL, Busby WF Jr, Thilly WG, Simoneit BRT (1998) Bioassay-directed chemical analysis of Los Angeles airborne particulate matter using a human cell mutagenicity assay. Environ Sci Technol 32:3502–3514
Hirose T, Morito K, Kizu R, Toriba A, Hayakawa K, Ogawa S, Inoue S., Muramatsu M, Masamune Y (2001) Estrogenic/antiestrogenic activities of benzo[a]pyrene monohydroxy derivatives. J Health Sci 47:552–558
IARC (1983) Polynuclear aromatic compounds. Part 1. Chemical, environmental and experimental data. IARC Monographs on the Evaluation of the Carcinogenic Risk of Chemicals to Humans. Vol. 32. IARC, Lyon, France
Iida M, Oguri H (2003) Japan patent 2003180393
Jones JM, Anderson JW (1999) Relative potencies of PAHs and PCBs based on the response of human cells. Environ Toxicol Pharmacol 7:19–26
Kamiya M, Toriba A, Onoda Y, Kizu R, Hayakawa K (2005) Evaluation of estrogenic activities of hydroxylated polycyclic aromatic hydrocarbons in cigarette smoke condensate. Food Chem Toxicol 43:1017–1027
Kannan K, Villneuve DL, Yamashita N, Imagawa T, Hashimoto S, Miyazaki A, Giesy JP (2000) Vertical profile of dioxin-like and estrogenic activities associated with a sediment core from Tokyo Bay, Japan. Environ Sci Technol 34:3568–3573
Kawanishi M, Takamura-Enya T, Ermawati R, Shimohara C, Sakamoto M, Matsukawa K, Matsuda T, Murahashi T, Matsui S, Wakabayashi K, Watanabe T, Tashiro Y, Yagi T (2004) Detection of genistein as an estrogenic contaminant of river water in Osaka. Environ Sci Technol 38:6424–6429
Kitamura S, Kato T, Iida M, Jinno N, Suzuki T, Ohta S, Fujimoto N, Hanada H, Kashiwagi K, Kashiwagi A (2005) Anti-thyroid hormonal activity of tetrabromobisphenol A, a flame retardant, and related compounds: affinity to the mammalian thyroid hormone receptor, and effect on tadpole metamorphosis. Life Sci 76:1589–1601
Kizu R, Okamura K, Toriba A, Kakishima H, Mizokami A, Burnstein KL, Hayakawa K (2003) A role of aryl hydrocarbon receptor in the antiandrogenic effects of polycyclic aromatic hydrocarbons in LNCaP human prostate carcinoma cells. Arch Toxicol 77:335–343
Kojima H, Iida M, Katsura E, Kanetoshi A, Hori Y, Kobayashi K (2003) Effects of a diphenyl ether-type herbicide, chlornitrofen, and its amino derivative on androgen and estrogen receptor activities. Environ Health Perspect 111:497–502
Lee B-C, Matsui S, Shimizu Y, Matsuda T (2005a) Characterization of the first flush in storm water runoff from an urban roadway. Environ Technol 26:773–782
Lee B-C, Shimizu Y, Matsuda T, Matsui S (2005b) Characterization of polycyclic aromatic hydrocarbons (PAHs) in different size fractions in deposited road particles (DRPs) from Lake Biwa area, Japan. Environ Sci Technol 39:7402–7409
Lee B-C, Matsui S, Shimizu Y, Matsuda T, Tanaka Y (2005c) A new installation for road runoff: up-flow filtration by porous polypropylene media. Water Sci Technol 52(12):225–232
Letzel T, Pöshl U, Wissiack R, Rosenberg E, Grasserbauer M, Niessner R (2001) Phenyl-modified reversed-phase liquid chromatography coupled ionization mass spectrometry: a universal method for the analysis of partially oxidized aromatic hydrocarbons. Anal Chem 73:1634–1645
Machala M, Vondráček J, Bláha L, Ciganek M, Neča J (2001a) Aryl hydrocarbon receptor-mediated activity of mutagenic polycyclic aromatic hydrocarbons determined using in vitro reporter gene assay. Mutat Res 497:49–62
Machala M, Ciganek M, Bláha L, Minksová K, Vondráčk J (2001b) Aryl hydrocarbon receptor-mediated and estrogenic activities of oxygenated polycyclic aromatic hydrocarbons and azaarenes originally identified in extracts of river sediments. Environ Toxicol Chem 20:2736–2743
Matsumoto H, Kashimoto T (1986) Embryotoxicity of organic extracts from airborne particulates in ambient air in the chicken embryo. Arch Environ Contam Toxicol 15:447–452
Mcdonald JD, Barr EB, White RK, Chow JC, Schauer JJ, Zielinska B, Grosjean E (2004) Generation and characterization of four dilutions of diesel engine exhaust for a subchronic inhalation study. Environ Sci Technol 38:2513–2522
Miller CA III (1999) A human aryl hydrocarbon receptor signaling pathway constructed in yeast displays additive responses to ligand mixtures. Toxicol Appl Pharmacol 160:297–303
Misaki K, Matsui S, Matsuda T (2007a) Metabolic enzyme induction by HepG2 cells exposed to oxygenated and nonoxygenated polycyclic aromatic hydrocarbons. Chem Res Toxicol 20:277–283
Misaki K, Kawami H, Tanaka T, Handa Y, Nakamura M, Matsui S, Matsuda T (2007b) Aryl hydrocarbon receptor ligand activity of polycyclic aromatic ketones and polycyclic aromatic quinones. Environ Toxicol Chem 26:1370–1379
Moore MN, Livingstone DR, Widdows J (1989) Hydrocarbons in marine mollusks: biological effects and ecological consequences. In: Varanasi U (ed) Metabolism of polycyclic aromatic hydrocarbons in the aquatic environment. CRC Press, Boca Raton, FL, pp 291–328
Nikolaou K, Masclet P, Mouvier G. (1984) Sources and chemical reactivity of polynuclear aromatic hydrocarbons in the atmosphere—a critical review. Sci Total Environ 32:103–132
Ohtake F, Takeyama K, Matsumoto T, Kitagawa H, Yamamoto Y, Nohara K, Tohyama C, Krust A, Mimura J, Chambon P, Yanagisawa J, Fujii-Kuriyama Y, Kato S (2003) Modulation of oestrogen receptor signalling by association with the activated dioxin receptor. Nature 423:545–550
Ohtake F, Baba A, Takada I, Okada M, Iwasaki K, Miki H, Takahashi S, Kouzmenko A, Nohara K, Chiba T, Fujii-Kuriyama Y, Kato S (2007) Dioxin receptor is a ligand-dependent E3 ubiquitin ligase. Nature 446:562–566
Okamura K, Kizu R, Toriba A, Murahashi T, Mizokami A, Burnstein KL, Klinge CM, Hayakawa K (2004) Antiandrogenic activity of extracts of diesel exhaust particles emmited from diesel-engine

truck under different engine loads and speeds. Toxicology 195:243–254

Pedersen DU, Durant JL, Taghizadeh K, Hemond HF, Lafleur AL, Cass GR (2005) Human cell mutagens in respirable airborne particles from the northeastern United States. 2. Quantification of mutagens and other organic compounds. Environ Sci Technol 39:9547–9560

Rogge WF, Hildemann LM, Mazurek MA, Cass GR (1993a) Sources of fine organic aerosol. 2. Noncatalyst and catalyst-equipped automobiles and heavy-duty diesel trucks. Environ Sci Technol 27:636–651

Rogge WF, Hildemann LM, Mazurek MA, Cass GR (1993b) Sources of fine organic aerosol. 3. Road dust, tire debris, and organometallic brakes lining dust: Roads as sources and sinks. Environ Sci Technol 27:1892–1904

Schmidt JV, Bradfield CA (1996) Ah receptor signaling pathways. Annu Rev Cell Dev Bioll 12:55–89

Till M, Riebniger D, Schmitz H-J, Schrenk D (1999) Potency of various polycyclic aromatic hydrocarbons as inducers of CYP1A1 in rat hepatocyte cultures. Chem-Biol Interact 117:135–150

Tsukue N, Toda N, Tsubone H, Sagai M, Jin WZ, Watanabe G, Taya K, Birumachi J, Suzuki AK (2001) Diesel exhaust (DE) affects the regulation of testicular function in male fischer 344 rats. J Toxicol Environ Health A 63:115–126

Tsukue N, Yoshida S, Sugawara I, Takeda K (2004) Effect of diesel exhaust on development of fetal reproductive function in ICR female mice. J Health Sci 50:174–180

van Lipzig MMH, Vermeulen ME, Gusinu R, Legler J, Frank H, Seidel A, Meerman JHN (2005) Formation of estrogenic metabolites of benzo[a]pyrene and chrysene by cytochrome P450 activity and their combined and supra-maximal estrogenic activity. Environ Toxicol Pharmacol 19:41–55

Vos JG, Dybing E, Greim HA, Ladefoged O, Lambre C, Terazona JV, Brandt I, Vethaak AD (2000) Health effects of endocrine-disrupting chemicals on wildlife, with special reference to the European situation. Crit Rev Toxicol 30:71–133

Watanabe N, Oonuki Y (1999) Inhalation of diesel engine exhaust affects spermatogenesis in growing male rats. Environ Health Perspect 107:539–544

Wells PG, Kim PM, Laposa RR, Nicol CJ, Parman T, Winn LM (1997) Oxidative damage in chemical teratogenesis. Mutat Res 396:65–78

Yoshida S, Sagai M, Oshio S, Umeda T, Ihara T, Sugamata M, Sugawara I, Takeda K (1999) Exposure to diesel exhaust affects the male reproductive system of mice. Int J Androl 22:307–315

Ziccardi MH, Gardner IA, Denison MS (2002) Application of the luciferase recombinant cell culture bioassay system for the analysis of polycyclic aromatic hydrocarbons. Environ Toxicol Chem 21:2027–2033

Available online at www.sciencedirect.com
ScienceDirect
Mutation Research 640 (2008) 27–37
Fundamental and Molecular Mechanisms of Mutagenesis
www.elsevier.com/locate/molmut
Community address: www.elsevier.com/locate/mutres

Differential effects of low- and high-dose X-rays on *N*-ethyl-*N*-nitrosourea-induced mutagenesis in thymocytes of B6C3F1 *gpt*-delta mice

Kazumi Yamauchi [a], Shizuko Kakinuma [a], Satomi Sudo [a,b], Seiji Kito [a], Yuki Ohta [a], Takehiko Nohmi [c], Ken-ichi Masumura [c], Mayumi Nishimura [a], Yoshiya Shimada [a,*]

[a] *Experimental Radiobiology for Children's Health Research Group, Research Center for Radiation Protection, National Institute of Radiological Sciences, 4-9-1, Anagawa, Inage-ku, Chiba 263-8555, Japan*
[b] *Department of Biomolecular Science, Faculty of Science, Toho University, 2-2-1, Miyama, Funabashi, Chiba 274-8510, Japan*
[c] *Division of Genetics and Mutagenesis, National Institute of Health Sciences, 1-18-1, Kamiyoga, Setagaya-ku, Tokyo 158-850, Japan*

Received 19 June 2007; received in revised form 30 November 2007; accepted 6 December 2007
Available online 15 December 2007

Abstract

Carcinogenesis in humans is thought to result from exposure to numerous environmental factors. Little is known, however, about how these different factors work in combination to cause cancer. Because thymic lymphoma is a good model of research for combined exposure, we examined the occurrence of mutations in thymic DNA following exposure of B6C3F1 *gpt*-delta mice to both ionizing radiation and *N*-ethyl-*N*-nitrosourea (ENU). Mice were exposed weekly to whole body X-irradiation (0.2 or 1.0 Gy), ENU (200 ppm) in the drinking water, or X-irradiation followed by ENU treatment. Thereafter, genomic DNA was prepared from the thymus and the number and types of mutations in the reporter transgene *gpt* was determined. ENU exposure alone increased mutant frequency by 10-fold compared to untreated controls and over 80% of mutants had expanded clonally. X-irradiation alone, at either low or high dose, unexpectedly, reduced mutant frequency. Combined exposure to 0.2 Gy X-rays with ENU dramatically decreased mutant frequency, specifically G:C to A:T and A:T to T:A mutations, compared to ENU treatment alone. In contrast, 1.0 Gy X-rays enhanced mutant frequency by about 30-fold and appeared to accelerate clonal expansion of mutated cells. In conclusion, repeated irradiation with 0.2 Gy X-rays not only reduced background mutation levels, but also suppressed ENU-induced mutations and clonal expansion. In contrast, 1.0 Gy irradiation in combination with ENU accelerated clonal expansion of mutated cells. These results indicate that the mode of the combined mutagenic effect is dose dependent.

Keywords: Combined genotoxic effect; *gpt*-delta mouse; *N*-Ethyl-*N*-nitrosourea; Radiation; Clonal expansion

1. Introduction

Humans are continuously and simultaneously exposed to numerous environmental mutagens. It is important, therefore, to determine the dose–effect relationship of combined exposure when assessing human health risks. Mutagenic DNA damage arises from interaction of DNA with a myriad of endogenous and exogenous agents [1]. Ionizing radiation induces DNA strand breaks and base modifications, directly or indirectly via reactive oxygen species. Such DNA damages result in base substitutions, insertions and deletions. Thus, the recent increase in the utilization of, and hence chance for exposure to, medical ionizing radiation has raised an aspect of social concern. Alkylating agents also modify DNA, thereby inducing base substitutions that lead to point mutations [2,3]. These agents are found in plants, food, cigarette smoke, fuel combustion products, and commonly used industrial solvents. In addition, ionizing radiation and some alkylating agents are used for cancer chemotherapy. *N*-Ethyl-*N*-nitrosourea (ENU) is a potent alkylating mutagen and carcinogen that induces G:C to A:T transitions,

* Corresponding author. Tel.: +81 43 206 3200; fax: +81 43 206 4138.
E-mail address: y_shimad@nirs.go.jp (Y. Shimada).

0027-5107/$ – see front matter © 2008 Elsevier B.V. All rights reserved.
doi:10.1016/j.mrfmmm.2007.12.001

A:T to G:C transitions and A:T to T:A transversions *in vivo* [4–8]. Since ionizing radiation and alkylating agents are widely distributed and utilized, understanding their toxicity and the cellular response mechanism(s) is important. Occasionally, we are exposed to these agents simultaneously in the environment or for therapeutic reasons. However, currently available data are not sufficient to delineate the mode and the mechanism of combined action of these agents.

The combined effect of radiation and alkylating agents has been examined in animal tumor models, including thymic lymphomas, brain tumors, mammary tumors and colon tumors [9–12]. Thymic lymphoma (TL) is an excellent model for human T-cell acute lymphoblastic leukemia and has been used for the study of radiation carcinogenesis. Concomitant exposure to butylnitrosourea and X-rays for 12 weeks accelerates the development of thymic lymphoma in BDF1 mice, in a manner dependent on the dose of radiation [9,13]. Irradiation 2–5 weeks before methylnitrosourea exposure accelerates thymic lymphoma development [13]. Irradiation for 5 days, but not 30 days, before administrating ENU treatment enhances lymphomagenesis [9].

DNA mutations play a central role in carcinogenesis. The frequency and type of mutations that result from combined treatment may shed light on the molecular mechanism(s) underlying the carcinogenic effects of combined exposure to alkylating agents and radiation. In order to delineate such mechanisms, we have examined the occurrence of mutations in thymic cells of B6C3F1 (*gpt+/−*) mice after combined exposure to X-rays and ENU. Repeated exposure to high-dose X-rays (1.0 Gy) followed by ENU increased the frequency of mutants and facilitated clonal expansion of mutated cells. However, unexpectedly, when low-dose X-rays (0.2 Gy) preceded ENU, mutant frequency was reduced primarily due to a decrease in G:C to A:T and A:T to T:A mutations. This is the first report, to our knowledge, that provides a new evidence on the mode and mechanism of combined exposure, which clearly differs between low and high dose of radiation.

2. Materials and methods

2.1. Mice

Male C3H/He mice were purchased from Charles River Laboratories (Kanagawa, Japan). Female *gpt*-delta C57BL/6J mice carrying approximately 80 copies of λEG10 DNA in haploid genome were obtained from Japan SLC (Shizuoka, Japan) [14]. Mice were housed five to a cage in a room maintained at 23 ± 2 °C and 50 ± 10% humidity, with a 12 h dark–light cycle. All mice were fed standard laboratory diet MB-1 (Funabashi Farm Co., Ltd., Chiba, Japan) and water *ad libitum*.

2.2. Chemicals

ENU (CAS No. 759-73-9) was purchased from Nakarai Tesque (Kyoto, Japan). Reagents for M9 buffer preparation were purchased from Nakarai Tesque and Wako Pure Chemical Industries (Osaka, Japan). Dimethyl sulfoxide and 6-thioguanine (6-TG) were purchased from Sigma Chemical Co. (St. Louis, MO, USA). Chloramphenicol (Cm) was purchased from Wako Pure Chemical Industries. Bacto yeast extract, Bacto tryptone and Bacto agar were obtained from Difco (Franklin Lakes, NJ, USA).

2.3. Irradiation

X-ray irradiation was performed using a Pantak HF-320 machine (PANTAK Ltd., East Haven, CT, USA) at 200 kV, 20 mA, and a dose rate of 0.7 Gy/min.

2.4. Combined X-ray exposure and ENU treatment

Mice (4–5 weeks old) were exposed weekly to 0.2 or 1.0 Gy X-rays for 4 consecutive weeks, because this X-ray exposure method is the most leukemogenic [15]. ENU was dissolved in reverse osmosis water (Elix UV10, Millipore, Bedford, MA) at pH 6.0 to prepare 200 ppm (1.17 mM) solution. To avoid degradation, ENU solution was administered in drinking water in brown bottle immediately after preparation. Freshly prepared ENU solution was exchanged on every Monday, Wednesday, Friday and Saturday during treatment. The amount of ENU solution up-taken was approximately 3 ml per mouse per day. For combined exposures, X-ray irradiation at 0.2 or 1.0 Gy for 4 consecutive weeks was followed by 4 weeks of ENU treatment (Fig. 1). Four weeks after the end of ENU treatment, mice were sacrificed and thymuses were collected and frozen immediately in liquid nitrogen, then stored at −80 °C until use. These animal experiments were conducted in compliance with guidelines for animal experiments of the National Institute of Radiological Sciences for the care and use of laboratory animals.

2.5. Genomic DNA extraction and in vitro packaging

The thymuses (20 mg) were homogenized in a Dounce homogenizer (Kontes, Vineland, NJ, USA) and genomic DNA was isolated using the RecoverEase DNA isolation kit (Stratagene, La Jolla, CA, USA). Transpack Packaging Extract (Stratagene, La Jolla, CA, USA) was used to rescue λEG10 phages from genomic DNA (10 μl) isolated from the thymus.

2.6. gpt mutation assay

The *gpt* mutagenesis assay was performed on five mice per group according to methods previously described [16]. Briefly, λEG10 phage was incubated with *E. coli* YG6020 at 37 °C for 20 min. After incubation, *E. coli* was incubated at 37 °C with vigorous agitation for 30 min. *E. coli* was mixed with 0.6% molten soft agar with or without 6-TG and the entire contents poured onto the M9 + Cm + 6-TG or M9 + Cm plates and incubated at 37 °C for 3 or 2 days. After incubation, colonies were counted and on M9 + Cm + 6-TG plates were subject to colony PCR for *gpt* gene. At least three independent experiments were performed per mouse.

Mutant frequency was calculated by dividing the number of colonies growing on M9 + Cm + 6-TG plates by the number of colonies growing on M9 + Cm plates.

Recurrent mutations derived from the same tissue of a single animal could be the result of clonal expansion that occurred early after mutagen treatment. When multiple identical mutations were recovered from an individual mouse, the

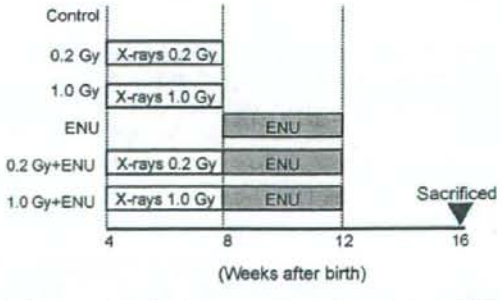

Fig. 1. Experimental design for *gpt* mutation analysis of thymic DNA from mice treated with X-ray irradiation, ENU or a combination of the two. Mice were exposed to X-rays weekly. ENU was administered at a concentration of 200 ppm in drinking water.

data were corrected for any clonal expressions by counting just the mutation as defined by independent mutation [17,18]. *Mutation frequency* was calculated as the ratio of calculated total independent mutants to the total number of colonies growing on M9 + Cm plates. Mutational common hot spots were defined as sites where the same mutation was observed in three or more mice from the same group. Clonality was calculated as the ratio of clonal (total − independent) mutations to the total mutations [19,20].

2.7. PCR and DNA sequencing analysis of gpt

A 739-bp DNA fragment containing *gpt* was amplified by PCR using two primers (primer 1 (forward): 5′-TACCACTTTATCCCGCGTCAGG-3′, primer 2 (reverse): 5′-ACAGGGTTTCGCTCAGGTTTGC-3′). The reaction mixture contained 5 pmol of each primer and 200 μM of each dNTP. PCR amplification was carried out using Taq DNA polymerase (Takara Bio, Shiga, Japan) with a GeneAmp PCR System 9700 (Applied Biosystems, Foster City, CA, USA). The reaction was started by incubation at 96 °C for 180 s, followed by 29 cycles of 30 s at 94 °C, 30 s at 58 °C, 60 s at 72 °C and an additional 180 s incubation at 72 °C after the final cycle.

PCR products were purified using Exo-SAP It (GE Healthcare Bio-Sciences Corp., Piscataway, NJ, USA). DNA sequencing of *gpt* was performed using Big Dye Terminator v3.1 (Applied Biosystems) on an ABI PRISM 3100 Genetic Analyzer (Applied Biosystems) with sequencing primer (5′-ATCTCTATAATCTCGCGCAACC-3′) according to the manufacturer's instructions. Oligonucleotide primers were obtained from Hokkaido System Science (Sapporo, Japan).

2.8. Statistical analysis

Mutant frequency is presented as mean ± S.D. Statistical significance was evaluated with the Student's *t*-test and Fisher's exact test using Graphpad Prism software (Graphpad Software Inc., San Diego, CA, USA). $P < 0.05$ was considered statistically significant.

3. Results

3.1. Thymus weight after treatment with ENU and X-rays

First, we measured body and thymus weight after combined exposure to X-rays and ENU (Table 1). The thymus weight of mice exposed to 0.2 or 1.0 Gy X-rays, ENU alone, or 0.2 Gy X-rays followed by ENU did not differ from that of non-irradiated controls. Thymus from mice exposed to 1.0 Gy X-rays followed by ENU weighed slightly greater than control thymus (68 ± 22 mg vs. 43 ± 9 mg; $P < 0.05$), suggestive of an onset of leukemogenesis. The body weight of all treated mice, except the 0.2 Gy followed by ENU mice, did not differ significantly from control.

3.2. Thymus gpt mutant frequency analysis

The *gpt* reporter transgene was used to analyze the occurrence of mutations in the thymus. The frequency of *gpt* mutants in each control and treated thymus is shown in Table 1 and Fig. 2. It is evident that ENU increased mutant frequency by 10-fold relative to untreated controls. Surprisingly, the mutant frequency in mice exposed to 0.2 or 1.0 Gy X-rays alone was significantly reduced compared to the control ($P < 0.05$). The mutant frequency in mice exposed to 0.2 Gy X-rays in combination with ENU was also, unexpectedly, reduced compared to ENU treatment alone, almost to the level of the untreated controls. In contrast, exposure

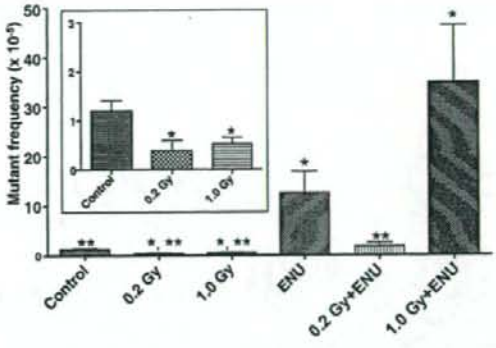

Fig. 2. Mutant frequency analysis of *gpt*⁻ recovered from thymus DNA from control, irradiated (0.2 or 1.0 Gy), ENU-treated, and irradiated/ENU-treated mice. The inset shows an expanded scale for mutant frequency for the first three conditions. * $P < 0.05$, significantly different from control. ** $P < 0.05$, significantly different from ENU. Bars represent mean ± S.D.

to 1.0 Gy X-rays in combination with ENU increased the mutant frequency by 3-fold compared to ENU treatment alone. In mouse #30 of ENU group, mutant frequency was not different from that in control group (0.91×10^{-5} vs. 1.20×10^{-5}), but the weight of thymus was significantly increased compared with control (Table 1). These results suggested that the thymocyte with no *gpt* mutation expanded in this mouse.

3.3. Characteristics of the gpt mutants

The class- and site-distribution of mutations are shown in Tables 2 and 3, respectively.

In control group, G:C to A:T mutation was predominantly detected, especially at both non-CpG and CpG sites (0.24×10^{-5} and 0.30×10^{-5}, respectively). In 0.2 and 1.0 Gy groups, however, G:C to A:T mutation at CpG was reduced by 6-fold compared to control, respectively (0.2 Gy, 0.05×10^{-5}; 1.0 Gy, 0.05×10^{-5}). In ENU group, G:C to A:T mutation was generated at non-CpG sites (8.26×10^{-5}) especially at positions 86 and 409. These sites might be hot spot for mutation by ENU, because four out of five mice commonly had these mutations. In addition, mutants with G:C to T:A and A:T to T:A in ENU group were also increased at the rate of 1.47×10^{-5} and 2.36×10^{-5}, respectively.

In 0.2 Gy followed by ENU group, however, the mutant frequency of G:C to A:T and A:T to T:A was significantly reduced compared to the ENU-treated group ($P < 0.001$). Particularly, mutants with G:C to A:T transitions decreased by 37-fold (ENU, 8.26×10^{-5}; 0.2 Gy + ENU, 0.24×10^{-5}).

In three mice of 1.0 Gy followed by ENU group, more than 1000 mutants were detected per thymus (#26, 27 and 29); 201, 168 and 135 mutants were analyzed for each mouse, respectively (Table 3). The class- and site-distribution of mutations differed between mice and jackpot mutation was shown. In mouse #26, 143 of 201 mutations were G:C to A:T transitions at position 87. Almost all of the mutations (164 of 168) detected in mouse #27 were A:T to C:G transversions at position 106 (Table 3). Ninety-eight of 135 mutations in mouse #29 were A:T to G:C transition

Table 1
Mutant and mutation frequency in thymus DNA from control, irradiated, ENU-treated, and combined treated mice

Treatment	Mouse ID	Body weight (g)	Average ± S.D. (mg)	Thymus weight (mg)	Average ± S.D. (mg)	Number of Cm colonies ($\times 10^5$)	Number of mutants	Mutant frequency ($\times 10^{-5}$)	Average ± S.D. ($\times 10^{-5}$)	Number of mutants sequenced	Number of independent mutants	Independent mutants (%)	Mutation frequency ($\times 10^{-5}$)	Average ± S.D. ($\times 10^{-5}$)
Control	1	25.7		45		18.3	32	1.75		28	22	79	1.38	
	2	25.8		39		12.7	16	1.26		14	13	93	1.17	
	3	24.6	26.5 ± 1.7	57	43 ± 9	16.2	21	1.30	1.2 ± 0.48	15	10	67	0.86	1.00 ± 0.43
	4	28.6		38		13.4	17	1.27		9	9	100	1.27	
	5	28.1		36		35.8	15	0.42		14	10	71	0.30	
	6	27.0		48		5.3	6	1.14		4	4	100	1.14	
	7	28.4		49		31.5	1	0.03		0	0	N.D.	N.D.	
0.2 Gy	8	24.6	26.3 ± 1.6	39	46 ± 6	28.3	4	0.14	0.39 ± 0.46*	1	1	100	0.14	0.59 ± 0.51[a]
	9	27.1		53		6.9	1	0.14		0	0	N.D.	N.D.	
	10	24.7		56		6.0	3	0.50		3	3	100	0.50	
	11	25.2		45		18.3	15	0.82		12	10	83	0.68	
	12	25.6		48		23.4	8	0.34		8	7	88	0.30	
1.0 Gy	13	24.6	25.0 ± 0.5	45	46 ± 1	47.8	12	0.25	0.53 ± 0.29*	9	9	100	0.25	0.49 ± 0.27
	14	24.5		45		15.0	13	0.87		10	10	100	0.87	
	15	25.5		47		8.5	3	0.35		2	2	100	0.35	
	16	24.5		35		17.7	110	6.21		110	15	14	0.85	
	17	26.7		43		2.3	66	28.21		58	12	21	5.84	
ENU	18	24.6	25.1 ± 1.0	36	41 ± 5	20.6	281	13.62	12.56 ± 9.67*	274	25	9	1.24	2.01 ± 2.15
	19	25.2		45		53.4	616	11.54		110	9	8	0.94	
	20	24.4		45		13.3	43	3.23		38	14	37	1.19	
	21	24.0		39		8.0	6	0.75		6	6	100	0.75	
	22	24.9		41		28.8	31	1.08		31	19	61	0.66	
0.2 Gy + ENU	23	24.6	24.4 ± 0.4*	35	40 ± 4	7.4	11	1.48	1.74 ± 1.76	10	9	90	1.34	1.12 ± 0.79
	24	24.8		47		5.0	24	4.82		22	11	50	2.41	
	25	24.0		38		31.3	18	0.57		17	13	76	0.44	
	26	24.4		64		18.5	1028	55.72		201	7	3	1.94	
	27	25.4		43		20.9	1001	47.94		168	5	3	1.43	
1.0 Gy + ENU	28	24.6	24.8 ± 0.9	100	68 ± 22*	5.7	75	13.09	34.74 ± 25.90*	59	8	14	1.77	1.61 ± 0.50
	29	25.9		54		27.5	1539	56.07		135	5	4	2.08	
	30	23.8		77		15.4	14	0.91		11	10	91	0.83	

N.D.: not determined.
[a] $n = 3$.
* $P < 0.05$, statistically significant difference vs. control.

Table 2
Classification and mutant frequency (M.F.) and mutation frequency (m.f.) of *gpt* mutations recovered from thymus DNA from control, irradiated, ENU-treated, and combined treated mice

	Control			0.2 Gy			1.0 Gy			ENU			0.2 Gy + ENU			1.0 Gy + ENU		
	No.	M.F. ($\times 10^{-5}$)	No.	m.f. ($\times 10^{-5}$)	No.	M.F. ($\times 10^{-5}$)	No.	m.f. ($\times 10^{-5}$)[a]	No.	M.F. ($\times 10^{-5}$)	No.	m.f. ($\times 10^{-5}$)	No.	M.F. ($\times 10^{-5}$)	No.	m.f. ($\times 10^{-5}$)	No.	M.F. ($\times 10^{-5}$)	No.	m.f. ($\times 10^{-5}$)
G:C to A:T (at non-CpG)	16	0.24	15	0.23	5	0.24	5	0.37	8	0.10	7	0.09	388	8.26	20	0.54	12	0.24	11	0.21	149	9.02	6	0.28
G:C to A:T (at CpG)[b]	20	0.30	11	0.17	1	0.05	1	0.07	4	0.05	3	0.04	1	0.02	1	0.03	7	0.14	5	0.10	5	0.30	4	0.18
G:C to T:A	16	0.24	15	0.23	0	<0.05	0	<0.07	12	0.16	12	0.15	69	1.47	15	0.40	15	0.30	10	0.19	20	1.21	4	0.18
G:C to C:G	3	0.05	3	0.05	0	<0.05	0	<0.07	1	0.01	1	0.01	2	0.04	2	0.05	0	<0.02	0	<0.02	1	0.06	1	0.05
Total G:C[c]	55	0.83	44	0.69	6	0.29	6	0.44	25	0.32	23	0.30	460	9.79	38	1.02	34	0.69	26	0.50	175	10.59	15	0.69
A:T to G:C	11	0.17	7	0.11	0	<0.05	0	<0.07	7	0.09	6	0.08	4	0.09	4	0.11	17	0.34	8	0.15	103	6.23	6	0.28
A:T to T:A	0	<0.02	0	<0.02	1	0.05	1	0.07	1	0.01	1	0.01	111	2.36	24	0.64	31	0.63	20	0.39	129	7.81	10	0.46
A:T to C:G	1	0.02	1	0.02	1	0.05	1	0.07	1	0.01	1	0.01	13	0.28	7	0.19	2	0.04	2	0.04	164	9.93	1	0.05
Total A:T[c]	12	0.18	8	0.13	2	0.10	2	0.15	9	0.12	8	0.10	128	2.72	35	0.94	50	1.01	30	0.58	396	23.97	17	0.78
1 bp deletion	6	0.09	6	0.09	0	<0.05	0	<0.07	6	0.08	6	0.08	2	0.04	2	0.05	1	0.02	1	0.02	2	0.12	2	0.09
1 bp insertion	2	0.03	2	0.03	0	<0.05	0	<0.07	1	0.01	1	0.01	0	<0.02	0	<0.02	1	0.02	1	0.02	1	0.06	1	0.05
>2 bp frameshifts	5	0.08	4	0.06	0	<0.05	0	<0.07	0	<0.01	0	<0.01	0	<0.02	0	<0.02	0	<0.02	0	<0.02	0	<0.06	0	<0.05
Total frameshifts	13	0.20	12	0.19	0	<0.05	0	<0.07	7	0.09	7	0.09	2	0.04	2	0.05	2	0.04	2	0.04	3	0.18	3	0.14
Total	80	1.20	64	1.00	8	0.39	8	0.59	41	0.53	38	0.49	590	12.56	75	2.01	86	1.74	58	1.12	574	34.74	35	1.61

No.: number of mutant(s). M.F.: specific mutant frequency was calculated by multiplying the mutant frequency by the ratio of the number of mutations in each class among the total number of *gpt* mutants. m.f.: specific mutation frequency was calculated by multiplying the mutation frequency by the ratio of independent mutation in each class to the total number of independent *gpt* mutant.

a $n = 3$.

b Number of occurrences of the G:C to A:T mutation at the 5′-CpG-3′ site.

c Total number of mutations occurring at G:C or A:T base pairs.

at position 419. These results indicate that the increased frequency of mutation in this group was caused by clonal expansion of cells possessing a unique mutation. None of the mutation sites were identical to those observed as hot spots in mice treated with ENU alone.

3.4. Mutation frequency

Unlike mutant frequency, difference in overall mutation frequency after ENU was calculated to be small among groups. However, A:T to T:A mutation frequency in ENU group, either combined or not combined with 1.0 Gy X-rays, was increased compared with control or X-ray irradiation groups (Table 2), while mutation at G:C sites remained unchanged statistically. The total mutation frequency by ENU group reduced from 2.01×10^{-5} to 1.12×10^{-5} when combined with 0.2 Gy, although statistically not significant. In contrast, repeated 1.0 Gy did not alter the overall frequency of ENU-induced mutation (1.61×10^{-5}).

3.5. Clonality of gpt mutations

The mutant frequency was significantly larger than mutation frequency in the groups treated with ENU alone, and with 1.0 Gy combined with ENU (Table 1). This means that mutation occurrence in ENU and 1.0 Gy combined with ENU groups were mainly caused by clonal expansion. We established the approximate level of clonality for each group. Clonality was less than 20% in the control group, which was the same as that observed in *lacI* transgenic mice [19]. Clonalities in 0.2 Gy X-ray and 1.0 Gy X-ray groups were also similar to that in the control group. It increased dramatically to over 80% in the ENU-treated group (Fig. 3). When 0.2 Gy X-ray exposure was combined with ENU, clonality was drastically reduced compared with ENU alone (24.6% vs. 82.2%, $P < 0.001$). In contrast, 1.0 Gy X-rays, except mouse #30, facilitated clonal expansion of mutated cells, as shown by the high percentage of subpopulations with specific mutations and the shift from an oligoclonal to monoclonal population (Table 3).

4. Discussion

In this study we investigated the combined effect of ENU and X-rays on the occurrence of mutations in the reporter transgene *gpt* in mouse thymus DNA. Repeated irradiation with 0.2 Gy X-rays not only reduced background mutation levels, but also suppressed ENU-induced mutations and clonal expansion. In contrast, 1.0 Gy irradiation in combination with ENU accelerated clonal expansion of mutated cells.

Reduction of the background mutation frequency by repeated dosing with 0.2 Gy X-rays or 1.0 Gy X-rays was unexpected. A decrease in G:C site mutations, including G:C to A:T at the CpG site, primarily accounted for this effect. The *gpt* in *gpt*-delta transgenic mice may be methylated at the CpG site [21]. Mammalian cell, in general, is heavily methylated at C-5 of cytosine residues at CpG dinucleotides. When 5-methylcytosine was deaminated, it converts to thymine, which results in G:C

Table 3
Mutational spectrum of *gpt* gene mutations recovered from thymus DNA from non-, X-ray-, ENU- and combined treated mice

Base positions[a]	CpG site	Control		0.2 Gy		1.0 Gy		ENU		0.2 Gy + ENU		1.0 Gy + ENU	
		No. of mutant	No. of independent mutation (mouse ID)	No. of mutant	No. of independent mutation (mouse ID)[b]	No. of mutant	No. of independent mutation (mouse ID)	No. of mutant	No. of independent mutation (mouse ID)	No. of mutant	No. of independent mutation (mouse ID)	No. of mutant	No. of independent mutation (mouse ID)
G:C to A:T													
3		2	2 (1, 4)										
7	CpG					1	1 (14)						
37		1	1 (5)										
58	CpG											1	1 (28)
64	CpG	12	4 (1,2,3, 5)	1	1 (6)	2	1 (11)			3	2 (21,25)		
86								194	4 (16,17,18,19)				
87								1	1 (18)			143	1 (26)
92				2	2 (6,8)					1	1 (22)	1	1 (26)
107		2	2 (1, 2)										
109	CpG	2	1 (5)										
110	CpG	1	1 (3)							3	2 (21,22)	2	1 (26)
113				1	1 (10)			2	2 (19,20)				
115	CpG	3	3 (2,3,4)			1	1 (12)	1	1 (17)	1	1 (22)	1	1 (27)
116								19	2 (16,18)				
128		1	1 (1)					83	2 (19,20)				
176						1	1 (11)	2	2 (17,19)				
189								1	1 (19)				
262						1	1 (12)						
274		2	2 (1,2)	1	1 (10)			1	1 (19)	1	1 (21)	2	1 (30)
280	CpG	1	1 (2)										
281		1	1 (1)			1	1 (15)					1	1 (30)
287								1	1 (16)				
301	CpG											1	1 (28)
391										1	1 (22)		
401				1	1 (6)	1	1 (13)			1	1 (22)		
402										2	2 (21,23)	1	1 (26)
406		3	2 (1,2)							1	1 (22)		
409								84	4 (16,17,18,19)			1	1 (26)
413	CpG	1	1 (2)										
417		1	1 (2)			1	1 (13)						
418		3	3 (1,2,5)			3	2 (11,12)			5	4 (22,23,24,25)		
Total at non-CpG		16	15	5	5	8	7	388*	20	12	11	149*	6
Total at CpG		20	11	1	1	4	3	1*	1	7	5	5*	4
G:C to T:A													
3												1	1 (30)
7	CpG					1	1 (11)	32	2 (16,18)				
15								1	1 (18)				
19	CpG									1	1 (24)		
26						1	1 (12)						
37						1	1 (13)						

79										1	1(27)
109	CpG	1	1 (4)								
110	CpG	1	1 (4)								
113						1	1 (16)				
115	CpG	1	1 (1)	1	1 (13)			1	1 (24)		
116		1	1 (3)	1	1 (15)	1	1 (16)				
143	CpG	1	1 (3)					1	1 (22)		
176				1	1 (14)						
185		1	1 (2)								
189								1	1 (23)		
190	CpG							1	1 (22)		
208	CpG					1	1 (18)	9	4 (22,23,24,25)	1	1(28)
232		1	1 (1)								
244	CpG	1	1 (5)	1	1 (13)	8	2 (18,19)				
265						3	2 (16,18)				
304		2	2 (1,2)								
401		1	1 (5)			19	3 (16,17,18)				
402		3	2 (1,5)	3	3 (11,13,14)						
406		1	1 (1)	1	1 (14)	1	1 (17)				
409		1	1 (1)			2	1 (17)	1	1 (24)	17	1(29)
418				1	1 (13)						
Total		16	15	12	12	69*	15	15	10	20*	4
G:C to C:G											
7	CpG					1	1 (17)			1	1(30)
115	CpG	1	1 (1)								
125	CpG					1	1 (18)				
289		1	1 (1)								
402				1	1 (15)						
436	CpG	1	1 (4)								
Total		3	3	1	1	2	2			1	1
A:T to G:C											
2		2	2 (4,5)							1	1(30)
8								1	1 (25)	1	1(29)
25		4	3 (1,2,4)								
56				1	1 (14)						
119								9	2 (22,25)		
149								1	1 (24)		
175				1	1 (11)						
181						1	1 (17)				
187						1	1 (17)			1	1(30)
188								1	1 (22)		
191								1	1 (21)	1	1(30)
269		2	1 (5)	1	1 (14)			1	1 (25)		
275										1	1(27)
277								3	1 (22)		
343				1	1 (14)						
419		3	1 (1)	3	2 (11,14)	1	1 (17)			98	1(29)
457						1	1 (18)				
Total		11	7	7	6	4	4	17	8	103*	6
A:T to T:A											
2						2	2 (18,19)	1	1 (25)		
12				1	1 (13)						
35								1	1 (25)	18	1(29)
52						5	2 (16,18)			1	1(27)
56						1	1 (18)				
81								1	1 (22)		
88						14	1 (19)	8	2 (23,24)	43	2(26, 28)
95								1	1 (25)		
134						16	4 (16,17,18,19)				

Table 3 (*Continued*)

Base positions[a]	CpG site	Control		0.2 Gy		1.0 Gy		ENU		0.2 Gy + ENU		1.0 Gy + ENU	
		No. of mutant	No. of independent mutation (mouse ID)	No. of mutant	No. of independent mutation (mouse ID)[b]	No. of mutant	No. of independent mutation (mouse ID)	No. of mutant	No. of independent mutation (mouse ID)	No. of mutant	No. of independent mutation (mouse ID)	No. of mutant	No. of independent mutation (mouse ID)
164				1	1(6)			3	3 (16,18,19)	2	2 (24,25)		
173								1	1 (18)				
177										1	1 (23)		
214										1	1 (24)		
223												1	1(30)
254												1	1(28)
257								2	1 (16)			1	1(28)
260										1	1 (25)		
263								8	2 (18,19)	7	3 (22,23,24)	63	2(26, 28)
312								1	1 (19)	2	1 (22)		
329								1	1 (18)			1	1(30)
345								56	4 (16,17,18,19)				
375										1	1 (22)		
400										2	2 (23,24)		
407										1	1 (23)		
420								1	1 (19)	1	1 (22)		
Total				1	1	1	1	111*	24*	31*	20*	129*	10*
A:T to C:G													
1								8	4 (16,17,18,19)				
9								1	1 (19)				
65				1	1(10)								
106								2	1 (19)			164	1(27)
218		1 (1)	1										
312										1	1 (25)		
331										1	1 (25)		
345						1	1 (14)	2	1 (18)				
Total		1	1	1	1	1	1	13	7	2	2	164*	1

No. of mutants: total number of mutations detected, include clonal mutations. Total number was shown the total number of mutations. No. of independent mutations: total number was shown the total number of independent mutations. The data were corrected for any clonal expansions by counting only one mutation when multiple identical mutations were recovered form an individual mouse. ID of mice with a mutation was shown in parentheses on the right-hand side of the total number of independent mutations.

[a] Position in the *gpt* coding sequence when A of start codon is labeled as 1.

[b] $n = 3$.

* $P < 0.05$ vs. control.

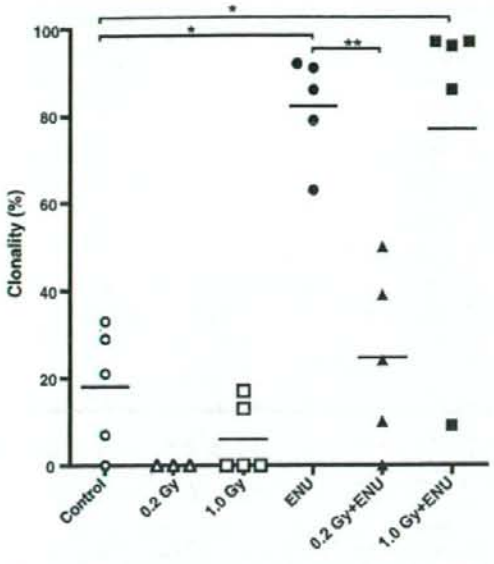

Fig. 3. Mutation clonality was enhanced by ENU as well as by 1.0 Gy X-rays in combination with ENU, but was suppressed by repeated irradiation with 0.2 Gy X-rays before ENU treatment. $^{*}P < 0.05$, significantly different from control. $^{**}P < 0.05$, significantly different from ENU. Bars represent means.

to A:T mutation after DNA replication if G:T mismatch is not repaired [22]. Repeated irradiation with 0.5 Gy X-rays leads to a decrease in DNA methylation via loss of histone H4-Lys20 trimethylation in thymus tissue [23], which could account for the reduced G:C to A:T mutation occurrence at CpG sites. Low-dose radiation (within 0.2 Gy) reduces thymic DNA fragmentation and apoptosis relative to non-irradiated background levels [24], suggesting that activation of DNA repair mechanisms may also contribute to the reduced frequency of mutations.

We show here that repeated 0.2 Gy irradiation also dramatically reduces ENU-induced mutations and the number of hot spot sites, primarily by decreasing the number of G:C to A:T transitions and G:C to T:A and A:T to T:A transversions. ENU produces ethylated base damage such as O^6-ethylguanine, O^4-ethylthymine and O^2-ethylthymine, which induces G:C to A:T transition, A:T to G:C transition and A:T to T:A transversion, respectively [4–8]. Base damage can be removed by multiple DNA repair systems. O^6-Methylguanine-DNA methyltransferase (*Mgmt*) recognizes and directly binds O^6-ethylguanine and removes the ethyl residue, thereby preventing G:C to A:T transition [25–28]. It is shown that transient expression of *Mgmt* is stimulated by X-irradiation both *in vitro* and *in vivo* within 3–48 h [29–31]. Importantly, the inductive effect of X-irradiation on O^6-alkylguanine-DNA alkyltransferase activity corresponds with a reduced incidence of rat CNS tumors after X-irradiation combination with ENU [10]. We have also examined if the expression of *Mgmt* mRNA increased after repeated X-irradiation of 0.2 Gy followed by ENU treatment. It turned out that the induction of *Mgmt* was negligible in irradiated thymus: fold increase was just 1.1 after the last irradiation. Subsequent ENU treatment increased *Mgmt* expression as a function of time. The 2-fold induction of *Mgmt* in thymus with 0.2 Gy followed by ENU, however, was smaller than 3.9-fold induction in thymus with ENU alone. Therefore, decrease in mutation frequency by 0.2 Gy could not be explained by expression level of *Mgmt*. Mechanism(s) other than *Mgmt* induction might be involved. Nucleotide excision repair can also repair alkylating base damage [32–34]. Chinese hamster ovary cells lacking *XPD/ERCC2* are highly susceptible to ENU-induced *Hprt* mutations [32]. DNA microarray studies indicate that *XPC* is up-regulated in human blood lymphocytes after 0.2 Gy X-ray exposure [35]. Taken together, it is required to determine activation or inactivation of other DNA repair pathways that reduce or enhance the overall rate of ENU-induced mutations.

We noticed that ENU mutations were predominantly induced at A:T site. It is reported that O^6-ethylguanine was repaired fast by *Mgmt* and nucleotide excision repair, while O^4-ethylthymine and O^2-ethylthymine were persistent lesions and the repair of these lesions occurred only at a very slow rate [25,32,36]. *In vivo* mutagenicity assays in mouse T lymphocytes have shown that predominant mutations induced by ENU are A:T to T:A [37].

Cells with hot spot point mutations expanded oligoclonally after ENU treatment. Clonal thymic lymphomas selected from oligoclonal preleukemic cells have been reported in virus-induced or radiation-induced T-cell lymphomagenesis [38,39]. Interestingly, the treatment with 0.2 Gy X-rays followed by ENU reduced oligoclonality, whereas 1.0 Gy X-rays accelerated ENU-induced clonal expansion. It is reported that high-dose whole body irradiation at 1.0 Gy induced p53 dependent transcription of *Noxa*, *Killer/DR5*, *Fas*, *Pidd* and *Perp* genes in thymus, whereas irradiation at 0.2 Gy did not induce these gene expressions [40]. Low-dose irradiation likely again activates multiple repair pathways and cell cycle control. In contrast, high-dose radiation may select specific clones with a growth advantage.

Point mutations of K-*ras*, *p53* and *Ikaros* occur frequently in ENU-induced T-cell lymphomas [41,42]. These mutations may enhance responsiveness of cells to growth factor induction of proliferation or resistance to apoptosis, thereby improving survival and increasing clonal expansion. When myeloma cells are cultured on normal bone marrow stromal cells, or in the presence of IL-6, activation of the K-*ras* oncogene provides a growth advantage over cells lacking activated K-*ras* [43]. The progression from low grade to high-grade brain tumors is associated with clonal expansion of cells that have acquired a *p53* mutation that endows the cells with a selective growth advantage [44]. T-cells with reduced or dominant-negative Ikaros activity, which may result from either a lack of or a point mutation in the zinc finger responsible for DNA binding, exhibit a greater proliferative response to IL-2 [45,46]. Irradiation of thymic epithelial cells enhances IL-7 production, and thymocytes at preleukemic stage proliferate more vigorously in response to IL-7 [47,48]. Taken together, these results suggest that high-dose radiation provides a thymic microenvironment ripe for the occurrence of prelymphoma cells, which harbor growth-advantageous mutations following ENU treatment.

In conclusion, low-dose X-rays (0.2 Gy) reduce not only the frequency of spontaneously occurring but also ENU-induced

mutations, suggestive of an adaptive response. Low-dose X-rays also reduce the clonal expansion of cells following ENU treatment, whereas 1.0 Gy X-rays accelerate cell expansion. Thus, low- and high-dose radiations play two different roles in lymphomagenesis when combined with ENU exposure.

Acknowledgements

We thank Dr. T. Shiomi, The Research Center for Charged Particle Therapy, National Institute of Radiological Sciences, and Dr. M. Ohta, Health Risk Assessment Section, National Institute for Environmental Studies, for technical advices. We also thank Ms. S. Amasaki, Ms. U. Enzaka, Ms. M. Okabe, Mr. J Nagai, Ms. S. Hirano and Ms. Y. Miyayama and the staff in Animal Facility of our institute for their assistance in laboratory analysis and mouse husbandry.

This work was supported in part by a grant from the Long-range Research Initiative (LRI) of the Japan Chemical Industry Association (JCIA), a grant from the 'Ground-based Research Announcement for Space Utilization' promoted by the Japan Space Forum, a grant from the Ministry of Health, Labour and Welfare, Japan, and a Grant-in-Aid from the Ministry of Education, Culture, Sports, Science, and Technology of Japan.

References

[1] E.C. Friedberg, G.C. Walker, W. Siede, R.D. Wood, R.A. Schultz, T. Ellenberger, DNA Repair And Mutagenesis, second edition, ASM Press, Washington DC, 2005.
[2] T. Shibuya, K. Morimoto, A review of the genotoxicity of 1-ethyl-1-nitrosourea, Mutat. Res. 297 (1993) 3–38.
[3] D.T. Beranek, Distribution of methyl and ethyl adducts following alkylation with monofunctional alkylating agents, Mutat. Res. 231 (1990) 11–30.
[4] J.C. Klein, M.J. Bleeker, J.T. Lutgerink, W.J. van Dijk, H.F. Brugghe, H. van den Elst, G.A. van der Marel, J.H. van Boom, J.G. Westra, A.J. Berns, et al., Use of shuttle vectors to study the molecular processing of defined carcinogen-induced DNA damage: mutagenicity of single O4-ethylthymine adducts in HeLa cells, Nucleic Acids Res. 18 (1990) 4131–4137.
[5] K.S. Ellison, E. Dogliotti, T.D. Connors, A.K. Basu, J.M. Essigmann, Site-specific mutagenesis by O6-alkylguanines located in the chromosomes of mammalian cells: influence of the mammalian O6-alkylguanine-DNA alkyltransferase, Proc. Natl. Acad. Sci. U.S.A. 86 (1989) 8620–8624.
[6] O.S. Bhanot, P.C. Grevatt, J.M. Donahue, C.N. Gabrielides, J.J. Solomon, In vitro DNA replication implicates O2-ethyldeoxythymidine in transversion mutagenesis by ethylating agents, Nucleic Acids Res. 20 (1992) 587–594.
[7] J.G. Jansen, G.R. Mohn, H. Vrieling, C.M. van Teijlingen, P.H. Lohman, A.A. van Zeeland, Molecular analysis of hprt gene mutations in skin fibroblasts of rats exposed in vivo to *N*-methyl-*N*-nitrosourea or *N*-ethyl-*N*-nitrosourea, Cancer Res. 54 (1994) 2478–2485.
[8] B. Singer, M.K. Dosanjh, Site-directed mutagenesis for quantitation of base–base interactions at defined sites, Mutat. Res. 233 (1990) 45–51.
[9] T. Seyama, T. Kajitani, A. Inoh, K. Yanagihara, K. Kamiya, K. Yokoro, Synergistic effect of radiation and *N*-nitrosoethylurea in the induction of lymphoma in mice: cellular kinetics and carcinogenesis, Jpn. J. Cancer Res. 76 (1985) 20–27.
[10] I. Stammberger, W. Schmahl, L. Nice, The effects of X-irradiation, *N*-ethyl-*N*-nitrosourea or combined treatment on O6-alkylguanine-DNA alkyltransferase activity in fetal rat brain and liver and the induction of CNS tumours, Carcinogenesis 11 (1990) 219–222.
[11] D.A. Kantorowitz, H.J. Thompson, P. Furmanski, Effect of high-dose, fractionated local irradiation on MNU-induced carcinogenesis in the rat mammary gland, Carcinogenesis 16 (1995) 649–653.
[12] Y. Morishita, T. Tanaka, H. Mori, S. Sasaki, Effects of X-irradiation on *N*-methyl-*N*-nitrosourea-induced multi-organ carcinogenesis in rats, Jpn. J. Cancer Res. 84 (1993) 26–33.
[13] H.J. Seidel, Effects of radiation and other influences on chemical lymphomagenesis, Int. J. Radiat. Biol. Relat. Stud. Phys. Chem. Med. 51 (1987) 1041–1048.
[14] T. Nohmi, M. Katoh, H. Suzuki, M. Matsui, M. Yamada, M. Watanabe, M. Suzuki, N. Horiya, O. Ueda, T. Shibuya, H. Ikeda, T. Sofuni, A new transgenic mouse mutagenesis test system using Spi- and 6-thioguanine selections, Environ. Mol. Mutagen. 28 (1996) 465–470.
[15] H.S. Kaplan, M.B. Brown, A quantitative dose–response study of lymphoid-tumor development in irradiated C 57 black mice, J. Natl. Cancer Inst. 13 (1952) 185–208.
[16] T. Nohmi, T. Suzuki, K. Masumura, Recent advances in the protocols of transgenic mouse mutation assays, Mutat. Res. 455 (2000) 191–215.
[17] S.E. Andrew, A.H. Reitmair, J. Fox, L. Hsiao, A. Francis, M. McKinnon, T.W. Mak, F.R. Jirik, Base transitions dominate the mutational spectrum of a transgenic reporter gene in MSH2 deficient mice, Oncogene 15 (1997) 123–129.
[18] J.C. Mirsalis, J.A. Shimon, A. Johnson, D. Fairchild, N. Kanazawa, T. Nguyen, J. de Boer, B. Glickman, R.A. Winegar, Evaluation of mutant frequencies of chemically induced tumors and normal tissues in lambda/cII transgenic mice, Environ. Mol. Mutagen. 45 (2005) 17–35.
[19] S. Zhang, B.W. Glickman, J.G. de Boer, Spontaneous mutation of the lacI transgene in rodents: absence of species, strain, and insertion-site influence, Environ. Mol. Mutagen. 37 (2001) 141–146.
[20] S. Zhang, R. Lloyd, G. Bowden, B.W. Glickman, J.G. de Boer, Thymic lymphomas arising in Msh2 deficient mice display a large increase in mutation frequency and an altered mutational spectrum, Mutat. Res. 500 (2002) 67–74.
[21] K. Masumura, M. Matsui, M. Katoh, N. Horiya, O. Ueda, H. Tanabe, M. Yamada, H. Suzuki, T. Sofuni, T. Nohmi, Spectra of *gpt* mutations in ethylnitrosourea-treated and untreated transgenic mice, Environ. Mol. Mutagen. 34 (1999) 1–8.
[22] B.K. Duncan, J.H. Miller, Mutagenic deamination of cytosine residues in DNA, Nature 287 (1980) 560–561.
[23] I. Pogribny, I. Koturbash, V. Tryndyak, D. Hudson, S.M. Stevenson, O. Sedelnikova, W. Bonner, O. Kovalchuk, Fractionated low-dose radiation exposure leads to accumulation of DNA damage and profound alterations in DNA and histone methylation in the murine thymus, Mol. Cancer Res. 3 (2005) 553–561.
[24] S.Z. Liu, Y.C. Zhang, Y. Mu, X. Su, J.X. Liu, Thymocyte apoptosis in response to low-dose radiation, Mutat. Res. 358 (1996) 185–191.
[25] S.M. Bronstein, T.R. Skopek, J.A. Swenberg, Efficient repair of O6-ethylguanine, but not O4-ethylthymine or O2-ethylthymine, is dependent upon O6-alkylguanine-DNA alkyltransferase and nucleotide excision repair activities in human cells, Cancer Res. 52 (1992) 2008–2011.
[26] M. Bignami, E. Dogliotti, G. Aquilina, A. Zijno, C.P. Wild, R. Montesano, O6-methyltransferase-deficient and -proficient CHO cells differ in their responses to ethyl- and methyl-nitrosourea-induced DNA alkylation, Carcinogenesis 10 (1989) 1329–1332.
[27] F. Drablos, E. Feyzi, P.A. Aas, C.B. Vaagbo, B. Kavli, M.S. Bratlie, J. Pena-Diaz, M. Otterlei, G. Slupphaug, H.E. Krokan, Alkylation damage in DNA and RNA-repair mechanisms and medical significance, DNA Repair (Amst.) 3 (2004) 1389–1407.
[28] A.E. Pegg, Repair of O(6)-alkylguanine by alkyltransferases, Mutat. Res. 462 (2000) 83–100.
[29] P. Lefebvre, F. Laval, Enhancement of O6-methylguanine-DNA-methyltransferase activity induced by various treatments in mammalian cells, Cancer Res. 46 (1986) 5701–5705.
[30] C.L. Chan, Z. Wu, A. Eastman, E. Bresnick, Irradiation-induced expression of O6-methylguanine-DNA methyltransferase in mammalian cells, Cancer Res. 52 (1992) 1804–1809.

[31] R.E. Wilson, B. Hoey, G.P. Margison, Ionizing radiation induces O6-alkylguanine-DNA-alkyltransferase mRNA and activity in mouse tissues, Carcinogenesis 14 (1993) 679–683.
[32] C.W. Op het Veld, S. van Hees-Stuivenberg, A.A. van Zeeland, J.G. Jansen, Effect of nucleotide excision repair on hprt gene mutations in rodent cells exposed to DNA ethylating agents, Mutagenesis 12 (1997) 417–424.
[33] J. Engelbergs, J. Thomale, A. Galhoff, M.F. Rajewsky, Fast repair of O6-ethylguanine, but not O6-methylguanine, in transcribed genes prevents mutation of H-ras in rat mammary tumorigenesis induced by ethylnitrosourea in place of methylnitrosourea, Proc. Natl. Acad. Sci. U.S.A. 95 (1998) 1635–1640.
[34] A. Sitaram, G. Plitas, W. Wang, D.A. Scicchitano, Functional nucleotide excision repair is required for the preferential removal of *N*-ethylpurines from the transcribed strand of the dihydrofolate reductase gene of Chinese hamster ovary cells, Mol. Cell. Biol. 17 (1997) 564–570.
[35] S.A. Amundson, K.T. Do, S. Shahab, M. Bittner, P. Meltzer, J. Trent, A.J. Fornace Jr., Identification of potential mRNA biomarkers in peripheral blood lymphocytes for human exposure to ionizing radiation, Radiat. Res. 154 (2000) 342–346.
[36] J.G. Jansen, C.M. van Teijlingen, G.R. Mohn, A.A. van Zeeland, H. Vrieling, AT base pairs are the main targets for mutations at the hprt locus of rat skin fibroblasts exposed in vitro to the monofunctional alkylating agent *N*-ethyl-*N*-nitrosourea, Mutagenesis 9 (1994) 417–421.
[37] J.P. O'Neill, DNA damage, DNA repair, cell proliferation, and DNA replication: how do gene mutations result? Proc. Natl. Acad. Sci. U.S.A. 97 (2000) 11137–11139.
[38] Y. Ben-David, E. Yefenof, M. Kotler, Clonal analysis of radiation leukemia virus-induced leukemic and preleukemic murine cells, Cancer Res. 47 (1987) 6590–6594.
[39] T. Shimizu, M. Muto, E. Kubo, T. Sado, H. Yamagishi, Multiple preneoplastic events and clonal selection of radiation induced mouse thymic lymphomas shown by TCR gene rearrangements, Leuk. Res. 17 (1993) 959–965.
[40] S. Alvarez, P. Drane, A. Meiller, M. Bras, V. Deguin-Chambon, V. Bouvard, E. May, A comprehensive study of p53 transcriptional activity in thymus and spleen of gamma irradiated mouse: high sensitivity of genes involved in the two main apoptotic pathways, Int. J. Radiat. Biol. 82 (2006) 761–770.
[41] Y. Shimada, M. Nishimura, S. Kakinuma, T. Takeuchi, T. Ogiu, G. Suzuki, Y. Nakata, S. Sasanuma, K. Mita, T. Sado, Characteristic association between K-ras gene mutation with loss of heterozygosity in X-ray-induced thymic lymphomas of the B6C3F1 mouse, Int. J. Radiat. Biol. 77 (2001) 465–473.
[42] S. Kakinuma, M. Nishimura, A. Kubo, J.Y. Nagai, Y. Amasaki, H.J. Majima, T. Sado, Y. Shimada, Frequent retention of heterozygosity for point mutations in p53 and Ikaros in *N*-ethyl-*N*-nitrosourea-induced mouse thymic lymphomas, Mutat. Res. 572 (2005) 132–141.
[43] D. Billadeau, P. Liu, D. Jelinek, N. Shah, T.W. LeBien, B. Van Ness, Activating mutations in the N- and K-ras oncogenes differentially affect the growth properties of the IL-6-dependent myeloma cell line ANBL6, Cancer Res. 57 (1997) 2268–2275.
[44] D. Sidransky, T. Mikkelsen, K. Schwechheimer, M.L. Rosenblum, W. Cavanee, B. Vogelstein, Clonal expansion of p53 mutant cells is associated with brain tumour progression, Nature 355 (1992) 846–847.
[45] N. Avitahl, S. Winandy, C. Friedrich, B. Jones, Y. Ge, K. Georgopoulos, Ikaros sets thresholds for T cell activation and regulates chromosome propagation, Immunity 10 (1999) 333–343.
[46] P. Papathanasiou, A.C. Perkins, B.S. Cobb, R. Ferrini, R. Sridharan, G.F. Hoyne, K.A. Nelms, S.T. Smale, C.C. Goodnow, Widespread failure of hematolymphoid differentiation caused by a recessive niche-filling allele of the Ikaros transcription factor, Immunity 19 (2003) 131–144.
[47] M. Nishimura, S. Kakinuma, D. Yamamoto, Y. Kobayashi, G. Suzuki, T. Sado, Y. Shimada, Elevated interleukin-9 receptor expression and response to interleukins-9 and -7 in thymocytes during radiation-induced T-cell lymphomagenesis in B6C3F1 mice, J. Cell Physiol. 198 (2004) 82–90.
[48] J. Toki, Y. Adachi, T. Jin, T. Fan, K. Takase, Z. Lian, H. Hayashi, M.E. Gershwin, S. Ikehara, Enhancement of IL-7 following irradiation of fetal thymus, Immunobiology 207 (2003) 247–258.

Mutation Research 673 (2009) 74–77

Contents lists available at ScienceDirect

Mutation Research/Genetic Toxicology and Environmental Mutagenesis

journal homepage: www.elsevier.com/locate/gentox
Community address: www.elsevier.com/locate/mutres

Short communication

Increased formation of gastric N^2-ethylidene-2′-deoxyguanosine DNA adducts in aldehyde dehydrogenase-2 knockout mice treated with ethanol

Haruna Nagayoshi[a,b], Akiko Matsumoto[c], Ryuhei Nishi[b], Toshihiro Kawamoto[d], Masayoshi Ichiba[c], Tomonari Matsuda[b,*]

[a] Osaka Prefectural Institute of Public Health, Osaka 537-0025, Japan
[b] Research Center for Environmental Quality Management, Kyoto University, Otsu 520-0811, Japan
[c] Department of Social and Environmental Medicine, Saga University, Saga 849-8501, Japan
[d] Department of Environmental Health, University of Occupational and Environmental Health, Kitakyusyu, Fukuoka 807-8555, Japan

ARTICLE INFO

Article history:
Received 2 September 2008
Received in revised form 7 October 2008
Accepted 22 November 2008
Available online 3 December 2008

Keywords:
Aldh2 knock-out mouse
Acetaldehyde
Stomach
LC/MS/MS
N^2-Ethylidene-2′-deoxyguanosine
N^2-Ethyl-2′-deoxyguanosine

ABSTRACT

We analyzed an acetaldehyde-derived DNA adduct, N^2-ethylidene-2′-deoxyguanosine (N^2-Eti-dG) in stomach DNA of aldehyde dehydrogenase (*Aldh*)-2-knockout mice that were fed with alcohol to determine effects of alcohol consumption and *Aldh2* genotype on the level of DNA damage in stomach. *Aldh2*-active(+/+), heterozygote(+/−) and knockout(−/−) mice were fed 20% ethanol for 5 weeks, then the level of N^2-Eti-dG in stomach was determined by liquid chromatography tandem mass spectrometry. The average N^2-Eti-dG level in DNA from untreated mice was not significantly different among *Aldh2* genotypes (2.0–3.1 adducts/10^7 bases), however, the average N^2-Eti-dG level in DNA from ethanol-treated mice was 4.8 ± 2.6 adducts/10^7 bases in *Aldh2*+/+ mice, 7.9 ± 1.1 adducts/10^7 bases in *Aldh2*+/− mice, and 48.6 ± 12.0 adducts/10^7 bases in *Aldh2*−/− mice, respectively. Our data clearly showed that alcohol drinking caused DNA damage in stomach, which was *Aldh2* genotype-dependent in this experimental animal model. This result suggests that heavy-alcohol drinking and *Aldh2* deficiency might be risk factors of stomach cancer.

1. Introduction

Alcohol intake is a risk factor for several types of cancer. Many studies of different design and in different populations around the world have consistently shown that daily alcohol consumption is a risk factor for cancers of oral cavity, pharynx, larynx and oesophagus [1–3]. Daily consumption of around 50 g of ethanol increases the risk for these cancers two to three times [1]. Moreover, many epidemiological studies consistently suggested that alcohol consumption is associated with an increased risk of liver cancer, breast cancer and colorectal cancer. In the case of stomach cancer, although many studies failed to show evidence of an association between alcohol drinking and stomach cancer risk, there are several other studies that clearly showed an association [4–7]. Endoscopic screening has yielded a higher rate of detection of gastric carcinoma in alcoholic Japanese men (1.7%) than in the general male Japanese population (0.2%) [8].

When the alcohol is assimilated, ethanol is metabolized and excreted in two steps. Firstly, ethanol is oxidized to acetaldehyde by alcohol dehyderogenase (ADH) and the ADH holoenzyme may exist as either a homodimer or heterodimer of α, β and γ subunits, encoded by *ADH1A*, *ADH1B* and *ADH1C*. The second step is the oxidation of acetaldehyde to acetate by aldehyde dehydrogenase (ALDH) or inducible cytochrome P450 2E1. Among human ALDH isozymes, the Michaelis constant (K_m) value of mitochondrial ALDH2 is predominantly low and that is why ALDH2 is a key enzyme for acetaldehyde metabolism. ALDH2 is a homotetrameric enzyme and the protein encoded by *ALDH2*2* has glutamic acid to lysin substitution at residue 487, resulting in an inactive subunit and dysfunctional ALDH2. ALDH2 has three types of polymorphism: *ALDH2*1/2*1*, an active form; *ALDH2*1/2*2*, a deficient form and *ALDH2*2/2*2* an inactive form. In *ALDH2*1/2*2* or *ALDH2*2/2*2* individuals, aldehyde remains in the body longer than in active *ALDH2*1/2*1* individuals and carcinogenic potential of acetaldehyde is exhibited [2,9].

Several reports described association between *ALDH2* genetic polymorphism and gastric cancers. Yokoyama and his colleagues reported that *ALDH2* genetic polymorphism was closely related with gastric cancer risk in Japanese alcoholic patients [10–12]. Chronic atrophic gastritis (CAG), which in many cases is induced

Abbreviations: ADH, alcohol dehydrogenase; ALDH, aldehyde dehydrogenase; N^2-Eti-dG, N^2-ethylidene-2′-deoxyguanosine; N^2-Et-dG, N^2-ethyl-2′-deoxyguanosine; CAG, chronic atrophic gastritis; α-*S*-Me-γ-OH-PdG, α-*S*-methyl-γ-hydroxy-1, N^2-propano-2′-deoxyguanosine; α-*R*-Me-γ-OH-PdG, α-*R*-methyl-γ-hydroxy-1, N^2-propano-2′-deoxyguanosine; 8-oxo-dG, 8-oxo-7,8-dihydro-2′-deoxyguanosine; LC/MS/MS, liquid chromatography tandem mass spectrometry.

* Corresponding author. Tel.: +81 75 753 5052; fax: +81 75 753 5052.
E-mail address: matsuda@z05.mbox.media.kyoto-u.ac.jp (T. Matsuda).

1383-5718/$ – see front matter © 2008 Elsevier B.V. All rights reserved.
doi:10.1016/j.mrgentox.2008.11.009